ONCOIMMUNOLOGY
2016, VOL. 5, NO. 11, e1239005 (14 pages)
http://dx.doi.org/10.1080/2162402X.2016.1239005

Taylor & Francis
Taylor & Francis Group

ORIGINAL RESEARCH

LAG-3 confers poor prognosis and its blockade reshapes antitumor response in head and neck squamous cell carcinoma

Wei-Wei Deng[a], Liang Mao[a], Guang-Tao Yu[a], Lin-Lin Bu[a], Si-Rui Ma[a], Bing Liu[a,b], J. Silvio Gutkind[c], Ashok B. Kulkarni[d], Wen-Feng Zhang[a,b], and Zhi-Jun Sun[a,b,d]

[a]The State Key Laboratory Breeding Base of Basic Science of Stomatology (Hubei-MOST) & Key Laboratory of Oral Biomedicine Ministry of Education, School and Hospital of Stomatology, Wuhan University, Wuhan, China; [b]Department of Oral Maxillofacial-Head Neck Oncology, School and Hospital of Stomatology, Wuhan University, Wuhan, China; [c]Department of Pharmacology, University of California, San Diego, CA, USA; [d]Functional Genomics Section, Laboratory of Cell and Developmental Biology, National Institute of Dental and Craniofacial Research, National Institutes of Health, Bethesda, MD, USA

ABSTRACT

Immunotherapy with immune checkpoint molecule-specific monoclonal antibody have obtained encouraging results from preclinical studies and clinical trials, which promoted us to explore whether this kind of immunotherapy could be applicable to head and neck squamous cell carcinoma (HNSCC). Lymphocyte activation gene-3 (LAG-3) is an immune checkpoint control protein that negatively regulates T cells and immune response. Here, using the human tissue samples, we report these findings that LAG-3 is overexpressed on tumor-infiltrating lymphocytes (TILs; $p < 0.001$) and its overexpression correlates with the high pathological grades, lager tumor size and positive lymph node status in human primary HNSCC. Survival analysis identifies LAG-3 as a prognostic factor independent of tumor size and pathological grades for primary HNSCC patients with negative lymph node status ($p = 0.014$). Study in immunocompetent genetically defined HNSCC mouse model reports that LAG-3 is upregulated on $CD4^+$ T cells, $CD8^+$ T cells and $CD4^+Foxp3^+$ regulatory T cells (Tregs). *In vivo* study, administration of LAG-3-specific antibody retards tumor growth in a way associated with enhanced systemic antitumor response by potentiating the antitumor response of $CD8^+$ T cells and decreasing the population of immunosuppressive cells. Taken together, our results offer a preclinical proof supporting the immunomodulatory effects of LAG-3 and suggest a potential therapeutic target of immunotherapy for HNSCC.

Abbreviations: aLAG-3, anti-mouse LAG-3 group; HNSCC, head and neck squamous cell carcinoma; LAG-3, lymphocyte activation gene-3; MDSCs, myeloid-derived suppressor cells; mLN, metastatic lymph nodes; OS, overall survival; PH, primary HNSCC; RH, recurrent HNSCC; RT, HNSCC with pre-radiotherapy history; TAMs, tumor-associated macrophages; TILs, tumor-infiltrating lymphocytes; TPF, HNSCC with inductive TPF chemotherapy; Tregs, regulatory T cells

ARTICLE HISTORY
Received 29 June 2016
Revised 14 September 2016
Accepted 15 September 2016

KEYWORDS
Antitumor response; head and neck squamous cell carcinoma; immunosuppressive cells; LAG-3; prognosis

Introduction

Head and neck squamous cell carcinoma (HNSCC) is one of the most common human malignancies and is frequently attributed to smoking, alcohol and human papillomavirus (HPV) infection.[1,2] Currently, HNSCC is characterized as a paradigm of immunosuppressive disease, with impaired function of effector cells, accumulated immunosuppressive cells and abnormalities in antigen-presenting function.[3] Discovery in cancer immunology has marked the arousal of increased interest toward the exploration and investigation of immunotherapy in HNSCC.[4]

Targeting inhibitory checkpoints such as PD-1 (programmed death-1) and CTLA-4 (cytotoxic T lymphocyte-associated antigen-4) has led to clinically encouraging antitumor response.[5,6] Lymphocyte activation gene-3 (LAG-3), one of the next generation of inhibitory checkpoints to be translated to the clinic, are highly expressed on exhausted or dysfunctional T cells in infection and cancer.[7] LAG-3 binds to major histocompatibility complex class II (MHC II) with a higher affinity than $CD4^+$.[8] Another ligand for LAG-3 is the LSECtin, which is a member of the C-type lectin receptor superfamily.[9] LSECtin is expressed on tumor cells and interacts with LAG-3 to limit the $CD8^+$ T cells signaling in melanoma.[10] The blockade of LAG-3 leads to increased accumulation and effector function of $CD8^+$ T cells in prostate cancer and ovarian cancer.[11,12] Recent studies have demonstrated that LAG-3 regulated inhibitory effect on T cells by collaborating with PD-1.[13,14] Meanwhile, clinical trial of LAG-3 monoclonal antibody (BMS-986016) alone and in combination with anti-PD-1 monoclonal antibody (Nivolumab, BMS-936558) for advanced solid tumors is currently recruiting participants.

Immunosuppressive cells, such as tumor-associated macrophages (TAMs), myeloid-derived suppressor cells (MDSCs) and regulatory T cells (Tregs), have been illustrated to be the key negative regulators of the immune system in various diseases including HNSCC.[15,16] Accumulation of these immunosuppressive cells during tumor progression could dampen T

CONTACT Zhi-Jun Sun sunzj@whu.edu.cn School and Hospital of Stomatology, Wuhan University, 237 Luoyu Road, Wuhan 430079, China.
Supplemental data for this article can be accessed on the publisher's website.

cells response and promote the development of tumor.[17-19] LAG-3 is expressed on Tregs and the blockade of LAG-3 could inhibit the activity of Tregs.[20] But whether the blockade of LAG-3 could reactivate the antitumor response of T cells and impact the immunosuppressive cells in HNSCC needs to be further proved.

We aimed to analyze the relationship of LAG-3 with clinicopathological parameters in HNSCC patients and to explore the alteration of tumor micro-environment (tumor) and macro-environment (spleen, lymph nodes and peripheral blood) in immunocompetent genetically defined HNSCC mouse model after the blockade of LAG-3.

Results

LAG-3 is highly expressed on tumor-infiltrating lymphocytes and correlated with high pathological grades, larger tumor size and positive lymph node status in human HNSCC

To determine whether LAG-3 expression was associated with human HNSCC, we examined the Tissue Cancer Genome Atlas (TCGA) dataset and Oncomine database. [21,22] In a meta-analysis of five datasets of head and neck cancer gene expression profiling for LAG-3, the LAG-3 gene expression was increased in HNSCC (Fig. S1A). And the DNA copy number and mRNA level of LAG-3 is significantly higher in HNSCC samples as compared with oral mucosa or blood (All $p < 0.05$; Figs. S1B–E). And immunofluorescence analysis in human HNSCC tissue sample detected expression and localization of LAG-3 predominantly in membrane of tumor-infiltrating lymphocytes (TILs), while there appeared to be some LAG-3 in the cytoplasm (Fig. S2). To further confirm the overexpression of LAG-3 in HNSCC, we perform immunohistochemical staining on human HNSCC tissue samples, which contains 27 oral mucosa, 43 dysplasia (Dys) and 122 primary HNSCC (PH) for LAG-3 with anti-LAG-3 antibody recognizing the aa 450 to the C-terminus. Consistently, LAG-3 expression on TILs was upregulated in tumor tissue compared with control oral mucosa (Fig. 1A). Of particular note, the high expression of LAG-3 was significantly associated with high pathological grade (I vs. II, $p < 0.05$), larger tumor size (T1 vs. T3, $p < 0.05$, T1 vs. T4, $p < 0.05$) and positive lymph nodes status (N0 vs. N1, $p < 0.05$; Fig. 1B). These results indicated that the LAG-3 expression on TILs correlates with advanced HNSCC.

Increased LAG-3 expression in human HNSCC is independent of HPV infection and other risk factors

HPV has been identified as the causative agent of subgroup of HNSCC.[23] To determine whether LAG-3 expression was correlated with HPV infection, we examined the expression of LAG-3 in HPV negative (HPV−) group and HPV positive (HPV+) group. P16 immunostaining and DNA *in situ* hybridization technique were used to monitor HPV infection as previously reported.[24] As shown in Fig. S3A, no difference of LAG-3 expression was found between and HPV− subgroup or HPV+ subgroup. To further identify this result, paired *t* test was used to eliminate the influence of TNM stage and pathological grades. Similarly, there was no significant difference in LAG-3 expression observed between HPV− group and HPV+ group (Fig. S3B). Additionally, we searched for HPV-related HNSCC TCGA dataset and Oncomine database.[21,22] There were no significant differences in the LAG-3 DNA copy number or the mRNA level in HPV-related HNSCC (All $p > 0.05$; Figs. S3C–E). Besides, we further investigated the association of LAG-3 with other risk factors. And no significant association was found between the expression of LAG-3 and alcohol consumption, cigarette smoking, age or gender in primary HNSCC (All $p > 0.05$; Table S1). These observations revealed that the expression of LAG-3 on TILs is a common event in human primary HNSCC.

LAG-3 expression is upregulated in recurrent HNSCC, metastatic lymph nodes and HNSCC with pre-radiotherapy

The majority of HNSCC patients with recurrence and metastasis remain poor outcomes, indicating the urgent need to develop novel therapeutic strategies that prolong survival and optimize quality of life.[25] Immunotherapy for HNSCC disrupting PD-1/PD-L1 axis has yielded encouraged responses, which seem to be durable in patients with refractory disease.[25] In the present study, the expression of LAG-3 significantly increased in recurrent HNSCC (RH, $n = 8$, $p < 0.001$; Fig. 1C), metastatic lymph nodes (LN, $n = 41$, $p < 0.001$; Fig. 1D) and pre-radiotherapy HNSCC specimen (RT, $n = 12$, $p < 0.05$; Fig. 1E) as compared to primary HNSCC (PH, $n = 122$). However, no significant association of LAG-3 expression was found between primary HNSCC and HNSCC with inductive TPF chemotherapy (TPF, $n = 11$, $p > 0.05$; Fig. 1F). These data suggest that LAG-3 expression on TILs may function in tumor recurrence and metastasis in HNSCC and targeting LAG-3 may be an effective approach in recurrent and metastatic HNSCC.

Highly expression of LAG-3 confers poor prognosis in human primary HNSCC with negative lymph node status

To further investigate the clinical significance of LAG-3 in human HNSCC, we explored the prognostic value of LAG-3. As shown in Table S2, we first confirm that the pathological grades, tumor size and lymph node status were significantly associated with poor prognosis in the present cohort of primary HNSCC patients. And a Kaplan–Meier curve showed that the primary HNSCC patients with high expression of LAG-3 ($LAG\text{-}3^{Hi}$) had borderline poor overall survival (OS) rate than those with low expression of LAG-3 ($LAG\text{-}3^{Lo}$; $p = 0.0739$; Fig. 1G). Furthermore, we investigated the prognostic value of the LAG-3 expression within primary HNSCC subgroups (pathological grades and TNM stage). Although we did not observe any significant differences in OS of patients subgrouping by pathological grades (Fig. S4A) and tumor size (Fig. S4B), the survival curve with high expression of LAG-3 was lower than the counterpart subgroup with low expression. More interestingly, in the patients with negative lymph node status (N^-), high infiltration of LAG-3 positive lymphocytes (N^{-Hi}) was significantly associated with poorer OS than low expression of LAG-3 (N^{-Lo}; $p = 0.0108$), but the survival curve of patients with positive lymph node status (N^+) did not differ (Fig. 1H).

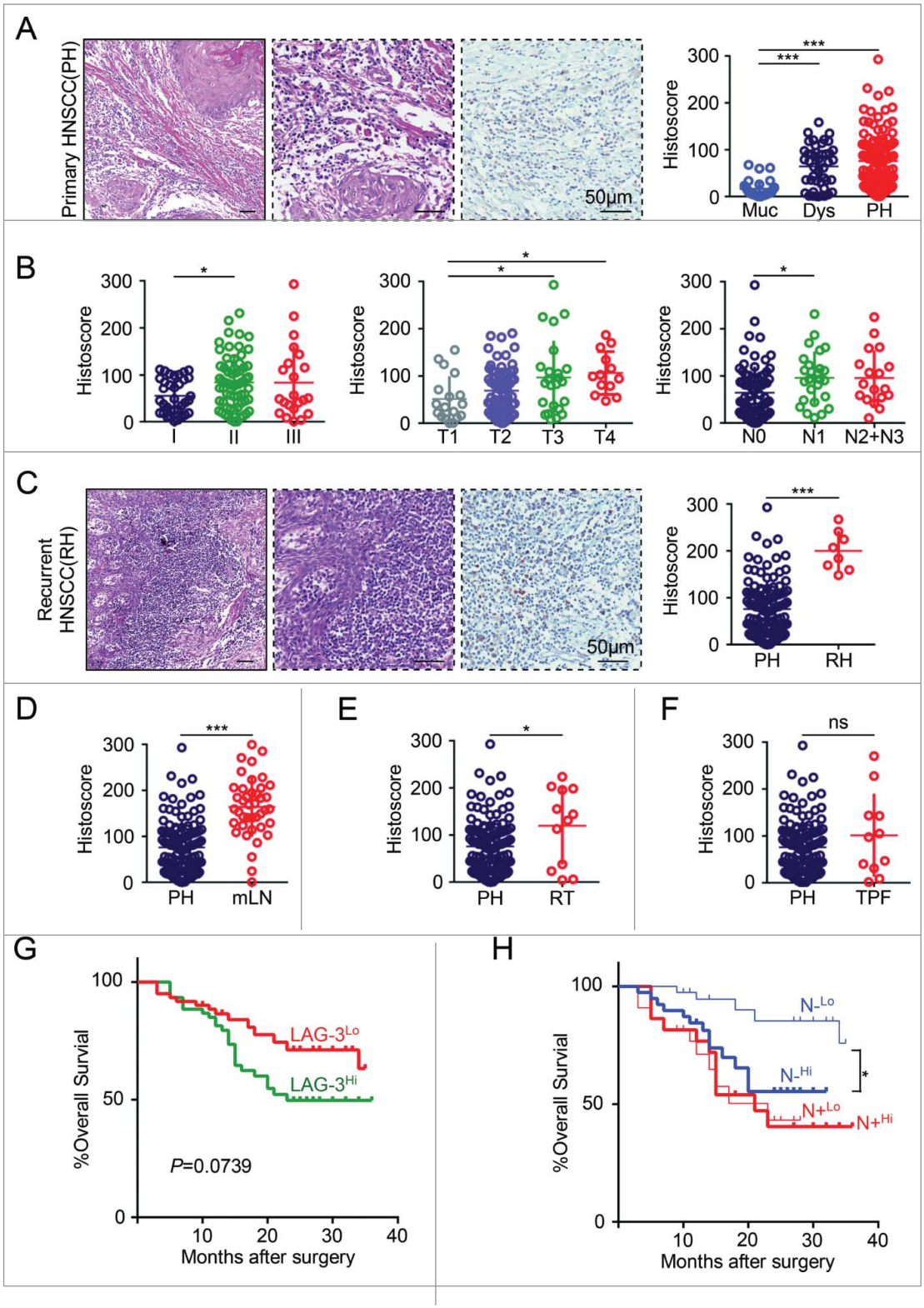

Figure 1. LAG-3 is highly expressed on tumor-infiltrating lymphocytes and correlated with clinicopathological parameters in human HNSCC. (A) Hematoxylin and Eosin (HE) staining and LAG-3 immunostaining of human primary HNSCC (PH) (left panel). Scale bar, 50 μm. The histoscore of LAG-3 expression in normal mucosa (Muc, n = 27), dysplasia (Dys, n = 43) and PH (n = 122) are quantified (right panel). Data were presented as Mean ± SEM, One-way ANOVA with post Tukey test, $^{***}p < 0.001$. (B) The quantitative analysis of LAG-3 histoscore is performed in pathological grades (I–III, left panel), tumor size (T1, T2, T3, T4, middle panel) and lymph node status (negative, N0; positive, N1, N2+N3, right panel), One-way ANOVA with post Tukey test, $^{*}p < 0.05$. (C) Representative images of HE and LAG-3 immunostaining in recurrent HNSCC (RH, left panel). Scale bar, 50μm.The quantitative analysis of LAG-3 histoscore in PH and RH (right panel). Unpaired *t* test, $^{***}p < 0.001$. The quantitative analysis of LAG-3 histoscore is performed in (D) metastatic lymph nodes (mLN vs. PH), (E) HNSCC with pre-radiotherapy history (RT vs. PH), or (F) HNSCC with inductive TPF chemotherapy (TPF vs. PH). Data is analyzed by unpaired *t* test, $^{*}p < 0.05$, $^{***}p < 0.001$, ns, no significance. *p* value and the number of each group or subgroup were displayed in Table S1. (G) Kaplan–Meier survival analysis and Log-rank test displayed overall survival (OS) of PH patients with high LAG-3 expression (LAG-3^{Hi}) vs. low LAG-3 expression (LAG-3^{Lo}). *p* (LAG-3^{Hi} vs. LAG-3^{Lo}) = 0.0739. (H) Prognostic role of LAG-3 expression level (High vs. Low) in PH with negative lymph node status (N^{-}) and positive lymph node status (N^{+}). *P* (N^{-Hi} vs. N^{-Lo}) = 0.0108; *p* (N^{+Hi} vs. N^{+Lo}) = 0.9229. All *p* value, Hazard ratio and 95% confidence interval were displayed in Table S2. For the variation of LAG-3 expression in different groups, all PH or PH subgroups were evenly categorized as LAG-3 high group and LAG-3 low group by the level of LAG-3 expression.

Table 1. Multivariate analysis for overall survival in primary HNSCC patients with negative lymph node status.

Parameters	HR (95%CI)	*p* value
Age	1.458 (0.417–5.094)	0.555
Grade		
I	1.000	1.000
II vs. I	8.202 (1.069–62.944)	0.043£
III vs. I	10.725 (1.186–96.971)	0.049£
Tumor size		
$T3^+T4$ vs. $T1^+T2$	2.101 (0.735–6.000)	0.166
LAG-3 expression		
High vs. low	4.160 (1.322–12.993)	0.014£

Note: Cox proportional hazards regression model.
HR: Hazard ratio; 95%CI: 95% confidence interval.
£ $p < 0.05$.

Furthermore, the multivariate analysis showed the high expression of LAG-3 on TILs was identified as an independent prognosis factor for OS ($p = 0.014$) in primary HNSCC patient with negative lymph node status (Table 1). These data indicated the expression of LAG-3 may indicate the poor prognosis in human primary HNSCC patients with negative lymph node status.

LAG-3 expression is closely correlated with $CD8^+$ and immunosuppressive cells in human HNSCC

On the basis of the closely relationship of LAG-3 with immunosuppressive status, we searched the publicly available database to explore whether LAG-3 is associated with $CD8^+$ and immunosuppressive cells markers. As mentioned *in silico* prediction of LAG-3 related genes by GenesLikeMe and STRING database, LAG-3 may correlate with s numerous immune molecules, such as $CD8^+$, Foxp3, CD33, CD11b (ITGAM), CD68 and CD163 (Table S3; Fig. S5). This result promotes us to analyze whether LAG-3 expression is associated with the expression of $CD8^+$, Tregs marker (Foxp3), human MDSCs markers (CD33 and CD11b) and M2-type TAMs markers (CD68 and CD163) in serial sections of HNSCC tissue samples (Fig. 2A). The Pearson's statistics results showed the expression of LAG-3 was positively correlated with $CD8^+$ ($p < 0.001$, $r = 0.3284$), Foxp3 ($p < 0.001$, $r = 0.3637$), CD33 ($p < 0.001$, $r = 0.3404$), CD11b ($p < 0.001$, $r = 0.2703$), CD68 ($p < 0.001$, $r = 0.2434$) and CD163 ($p < 0.001$, $r = 0.3056$) in oral mucosa ($n = 27$), dysplasia ($n = 43$) and primary HNSCC ($n = 122$; Fig. 2B). Hierarchical clustering analysis offered the intuitive intensity of correlation of LAG-3 with $CD8^+$, Foxp3, CD11b, CD33, CD68 and CD163 (Fig. 2C). Our data suggest that LAG-3 is closely correlated with $CD8^+$ and immunosuppressive cells in human HNSCC.

LAG-3 expression is significantly upregulated in Tgfbr1/Pten 2cKO mouse model

Both transforming growth factor-β (TGF-β) and PTEN/PI3K/Akt/mTOR pathways are frequently deregulated signaling routes in the oncogenesis of HNSCC.[26] *Pten* deletion in the mice head and neck epithelia give rise to the activation of PI3K/Akt pathway, and loss of *Tgfbr1* in the head and neck epithelia enhances paracrine effect of TGF-β on the tumor stroma.[27] Meanwhile, conditional deletion of *Pten* and *Tgfbr1* (2cKO) in head and neck epithelia could result in SCC in mice with complete penetrance and immunocompetent.[27] Given the multiple molecular alternation and pathology of the 2cKO mice tumor resembling human HNSCC, the 2cKO mouse model is suitable for studying the development of cancer and strategies for prevention of HNSCC, especially for immunotherapy.[24,28] To confirm the upregulation of LAG-3 in HNSCC mouse model, we quantified LAG-3 expression on $CD4^+$ and $CD8^+$ T cells by flow cytometry. As expected, the expression of LAG-3 in 2cKO tumor-bearing mice was dramatically elevated on both $CD4^+$ (Fig. 3A) and $CD8^+$ (Fig. 3B) T cells compared with WT mice. Given the close relationship of LAG-3 with immunosuppressive cells in human HNSCC samples, we also measured the expression of LAG-3 in $CD4^+Foxp3^+$ Tregs, $CD11b^+Gr1^+$MDSCs and $CD11b^+F4/80^+$ TAMs. And 2cKO tumor-bearing mice had a higher proportion of $LAG\text{-}3^+$ cells on Tregs compared with WT mice (Fig. 3C). However, results reported in Fig. 3D and E showed that MDSCs and TAMs expressed extremely low level of LAG-3. We then evaluated LAG-3 expression in lymphocytes by flow cytometry in wild-type (WT) mice and 2cKO tumor-bearing mice. The result showed that LAG-3 expression was significantly higher in 2cKO tumor-bearing mice compared with WT mice (Fig. S6A). We further investigated the expression of LAG-3 on lymphocytes of the mouse tumor, using paraffin-embedded tissue sections. As shown in the representative images (Fig. S6B), positive LAG-3 staining was observed in the 2cKO HNSCC but not the WT tongue mucosa. Similar to immunohistochemistry, the Western blot showed a gradually increased protein level of LAG-3 in WT tongue, 2cKO mice tongue and 2cKO mice tongue squamous cell carcinoma (TSCC; Fig. S6C). These findings suggested that LAG-3 was increased in 2cKO tumor-bearing mice. We speculated that the upregulation of LAG-3 during tumor progression might reflect the immunosuppressive status and blockade of LAG-3 might enhance antitumor response and retard tumor growth.

The blockade of LAG-3 retards tumor growth in HNSCC mouse model

To validate the efficacy of the blockade of LAG-3 *in vivo*, we tested the chemopreventive effect of the blockade of LAG-3 in the immunocompetent *Tgfbr1/Pten* 2cKO mouse model. As schematically shown in Fig. 4A, tamoxifen was applied to *Tgfbr1*$^{flox/flox}$; *Pten*$^{flox/flox}$; *K14-CreER*$^{tam+/-}$ *mice* by oral gavage in five consecutive days for the conditional deletion of *Tgfbr1* and *Pten* in head and neck epithelia, resulting in HNSCC.[29] A week later, *in vivo* anti-mouse LAG-3 antibody (aLAG-3 group, clone: C9B7W; 10 mg/kg) or isotype control (control group, clone: MOPC-21; 10 mg/kg) was infused by intraperitoneal injection every other day for next 10 d (Fig. 4A). Based on the measurements of tumor volume, the tumor growth was mainly restricted in the head neck area (Fig. 4B; quantification in Fig. 4C). Likewise, administration of aLAG-3 delayed the tongue tumor development and growth (Fig. 4B). The cytotoxicity of antibody was evaluated by the weight of mice being treated and the less toxicity was observed in aLAG-3 group as indicated by a slight gain of weight as compared with significant loss of weight in control group ($p < 0.01$; Fig. 4D). The expression of LAG-3 was

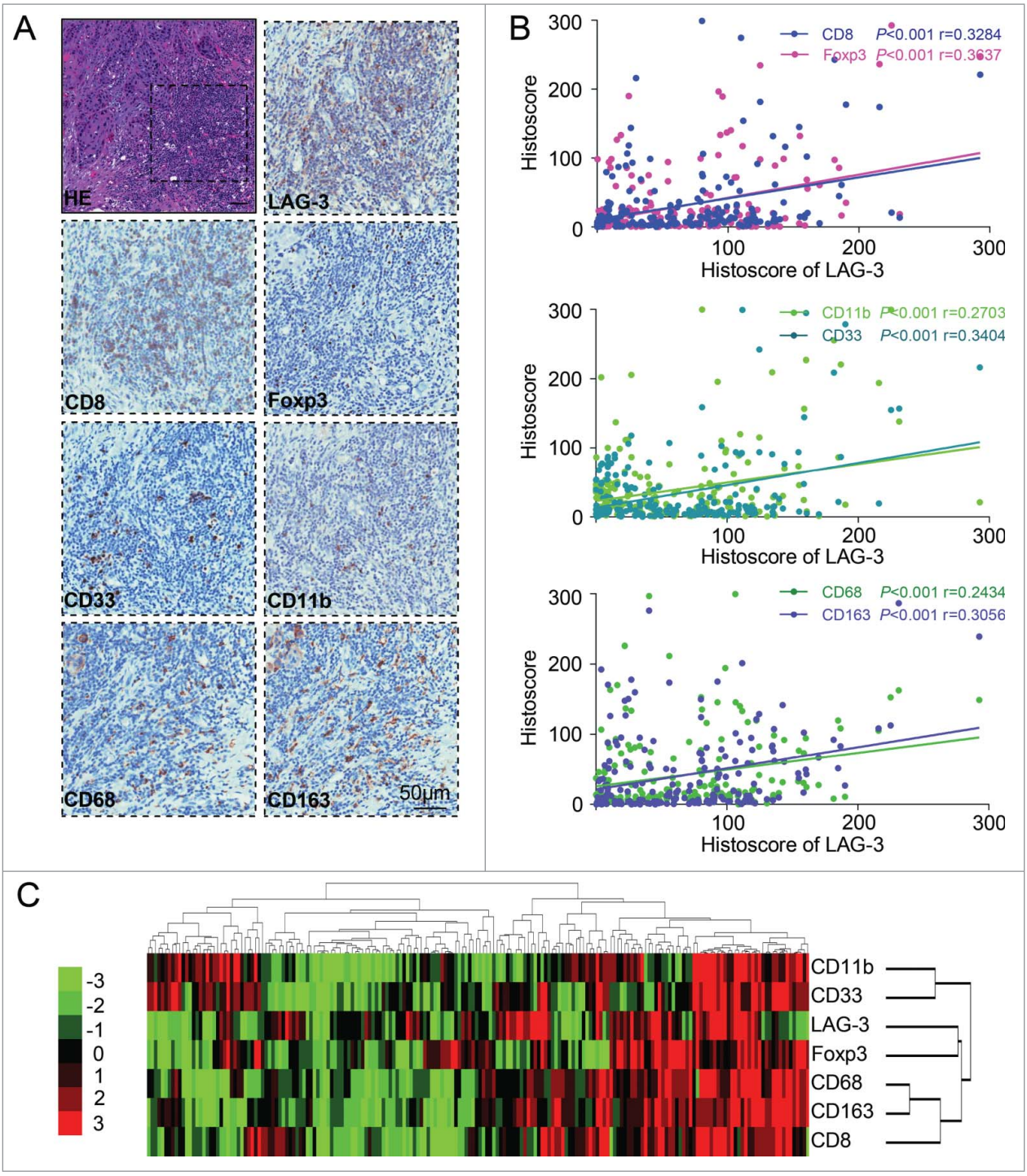

Figure 2. LAG-3 expression is closely associated with $CD8^+$ and immunosuppressive cells in human HNSCC. (A) Representative HE and immunohistochemical staining of LAG-3, $CD8^+$, Foxp3, CD33, CD11b, CD68 and CD163 in serial sections of HNSCC tissue samples. Scale bar, 50 μm. (B) The Spearman rank correlation coefficient test and linear tendency test showed that LAG-3 was positively correlated with $CD8^+$ ($p < 0.001$, r = 0.3284), Foxp3 ($p < 0.001$, r = 0.3637), CD11b ($p < 0.001$, r = 0.2703), CD33 ($p < 0.001$, r = 0.3404), CD68 ($p < 0.001$, r = 0.2434) and CD163 ($p < 0.001$, r = 0.3056) in oral mucosa (n = 23), dysplasia (n = 47) and primary HNSCC (n = 122). (C) Hierarchical clustering presented the correlation of LAG-3, $CD8^+$, Foxp3, CD11b, CD33, CD68 and CD163 expression in oral mucosa, dysplasia and primary HNSCC.

distinctly reduced as indicated by flow cytometry (Fig. 4E), Western blot (Fig. 4F) and immunostaining (Fig. 4G) in aLAG-3 group as compared with control group, which indicate the possible on-target effect of LAG-3 blockade. Taken together, these data supported that the blockade of LAG-3 suppressed the tumor development in immunocompetent HNSCC mouse model.

The blockade of LAG-3 potentiates antitumor response of $CD8^+$ T cells in HNSCC mouse model

Given the downregulated $CD4^+$ and $CD8^+$ T cells in 2cKO tumor-bearing mice during carcinogenesis, we examined whether the blockade of LAG-3 affected $CD4^+$ and $CD8^+$ T

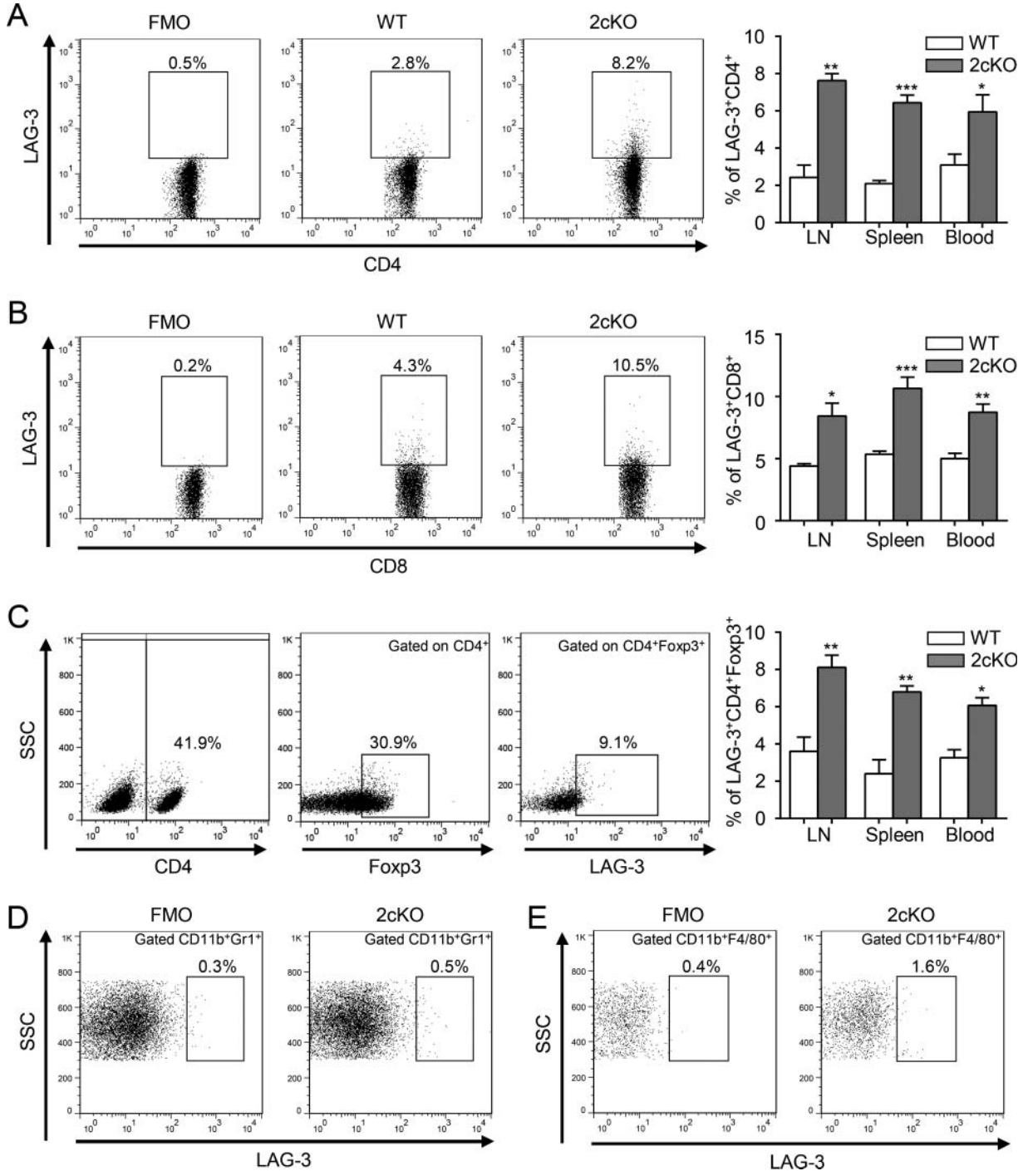

Figure 3. LAG-3 expression is significantly upregulated in HNSCC mouse model. (A, B) Dot plots showed the expression of LAG-3 in the (A) $CD4^+$ gated population and (B) $CD8^+$ gated population. The percentage of LAG-3 in the $CD4^+$ gated population and $CD8^+$ gated population compared between WT mice and 2cKO tumor-bearing mice were shown in bar graph. Cells were harvested from LN, spleen and peripheral blood. Data are shown as Mean ± SEM. $^*p < 0.05$, $^{**}p < 0.01$, $^{***}p < 0.001$. (C) The gating strategy for LAG-3 in $CD4^+$ $Foxp3^+$ gated population (left panel). The percentage of LAG-3^+ cells in $CD4^+Foxp3^+$ gated population compared between WT mice and 2cKO tumor-bearing mice were shown in bar graph. Cells were harvested from LN, spleen and peripheral blood. Data are shown as Mean ± SEM. $^*p < 0.05$, $^{**}p < 0.01$. (D, E) Flow cytometry plots of (D) $CD11b^+Gr1^+$ gated population and (E) $CD11b^+F4/80^+$ gated population subjected to isotype control (left panel) and LAG-3 (right panel) in 2cKO tumor-bearing mice.

cells. The blockade by aLAG-3 treatment resulted in a significantly increased percentage of $CD8^+$ T cells in spleen, lymph nodes and tumors as compared with control (Figs. 5A and B). We next tested whether the blockade of LAG-3 could enhance $CD8^+$ T cells response. As shown in Fig. 5C, the blockade of LAG-3 significantly enhanced IFNγ^+CD8^+ T cells responses compared with control. Indeed, the $CD4^+$ T cell population decreased in tumor-bearing mice as compared with WT counterpart. The comparison of control group with the aLAG-3 group did not highlight any significant differences in the percentage of $CD4^+$ T cells, although a slightly higher variation is observable within the aLAG-3 group (Fig. 5D). We also observed the enlarged lymph nodes (Fig. 5E) and splenomegaly (Fig. 5F) in 2cKO tumor-bearing mice by gross biopsy, which indicated an immune dysregulation. The size of spleen and lymph nodes, to some extent, could be reduced after the

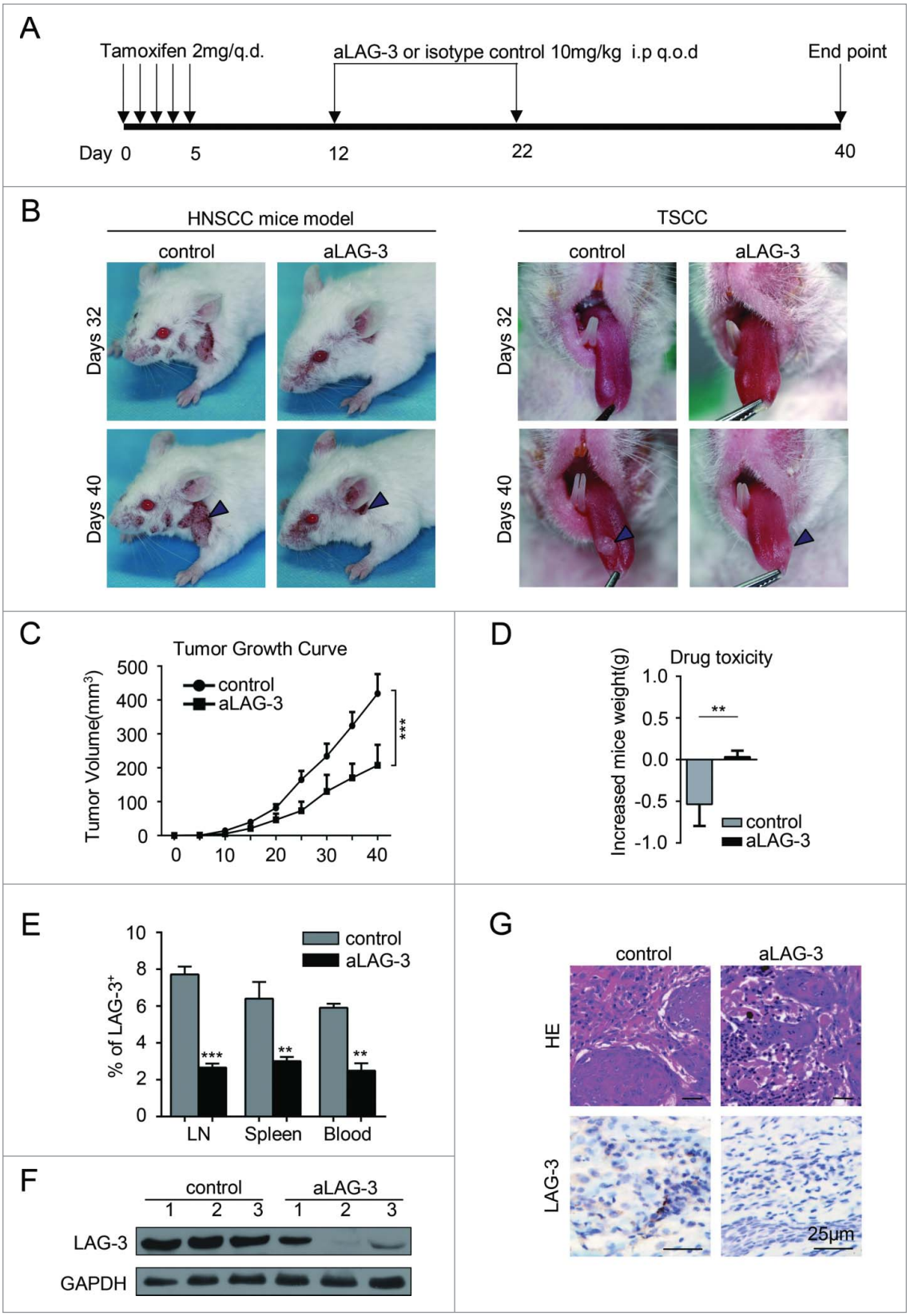

Figure 4. Anti-mLAG-3 (aLAG-3) retards tumor growth in HNSCC mouse model. (A)Schematic image showed the chemopreventive therapeutic strategy for HNSCC mouse model. *Pten/Tgfbr1* 2cKO mice randomly were divided into two groups and treated with isotype control (control group, *in vivo* MAb mouse IgG1 isotype control, Clone: MOPC-21; Bioxcell; n = 6 mice; 10 mg/kg) and anti-mouse LAG-3 group (aLAG-3 group, *in vivo* mAb LAG-3 antibody, Clone: C9B7W, Bioxcell; n = 6 mice; 10 mg/kg). (B) Representative images of HNSCC (left panel) and tongue squamous cell carcinoma (TSCC, right panel) in control group and aLAG-3 group at days 32 and days 40. The arrow head illustrated HNSCC and TSCC. (C)Tumors were measured with the electronic caliper and presented as tumor volume. Six mice per group. $^{***}p < 0.001$. (D) The drug toxicity was evaluated by gained weight of control group and aLAG-3 group. $^{**}p < 0.01$. (E) The blockade of LAG-3 reduced the population of LAG-3^{+} cells. Data are shown as Mean ± SEM. $^{**}p < 0.01$, $^{***}p < 0.001$. (F) Western blot showed the LAG-3 protein level in control group and aLAG-3 group. (G) Representative image of HE (upper panel) and LAG-3 immunostaining (lower panel) in tumors from control mice or aLAG-3 mice. Scale bar, 25 μm.

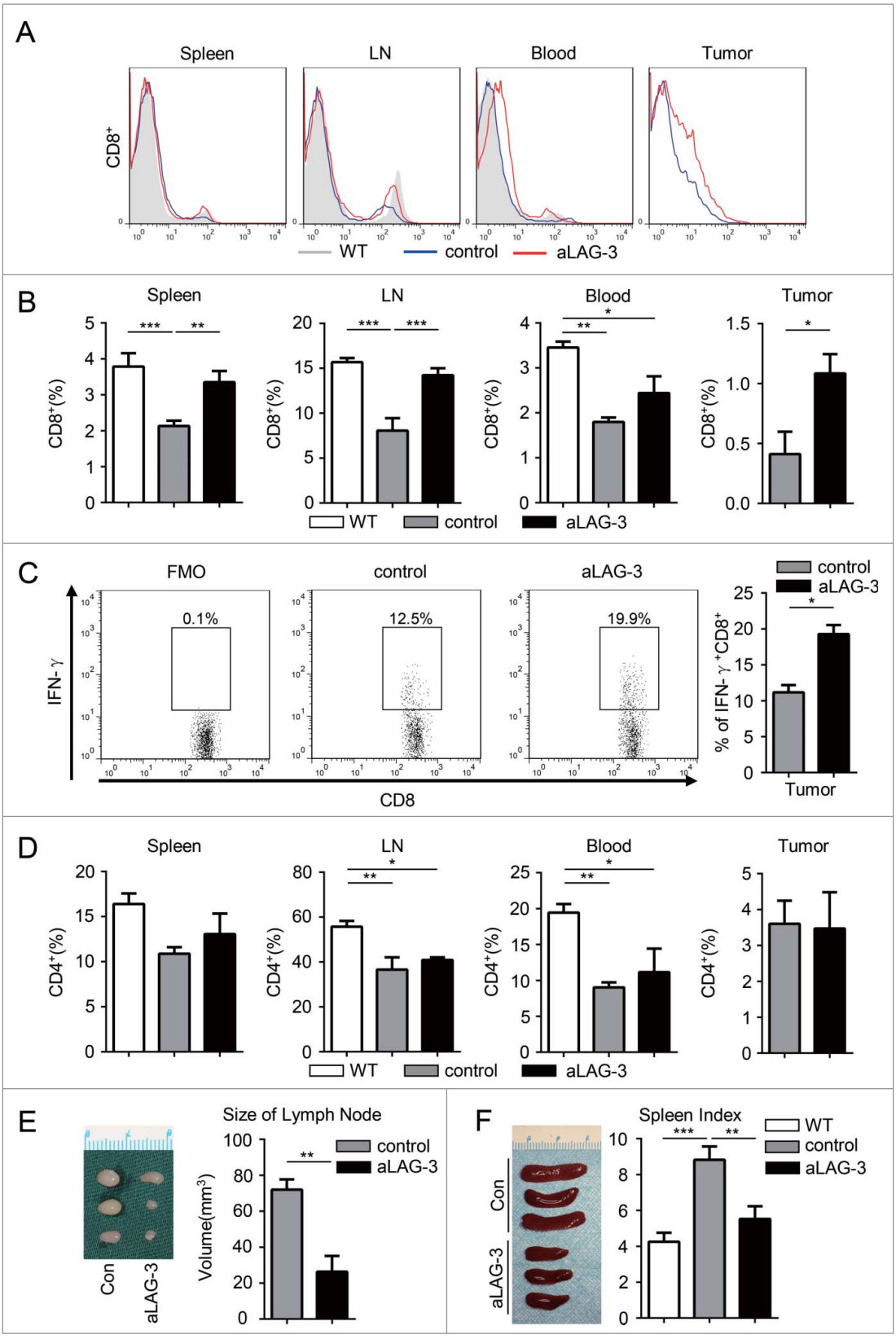

Figure 5. The blockade of LAG-3 (aLAG-3) enhanced the antitumor response of $CD8^+$ T cells in HNSCC mouse model. (A) Histogram and (B) quantification of $CD8^+$ T cells population in WT mice, control mice and aLAG-3 mice. Cells were harvested from spleen, lymph node (LN), peripheral blood and tumor tissues. The percentage of $CD8^+$ T cells is the proportion of $CD8^+$ T cells accounting for the number of the total viable cells. Data are shown as Mean ± SEM. $^*p < 0.05$, $^{**}p < 0.01$, $^{***}p < 0.001$. (C) Representative flow cytometric plots and the percentage of $IFN\gamma^+CD8^+$ T cells population in tumor-infiltrating lymphocytes (TILs) from control group and aLAG-3 group. Data presented as Mean ± SEM. $^*p < 0.05$. (D) Quantitative analysis of the percentage of $CD4^+$ T cells in WT group, control group and aLAG-3 group. Cells were harvested from spleen, LN, peripheral blood and tumor tissues. The percentage of $CD4^+$ T cells is the proportion of $CD4^+$ T cells accounting for the number of the total viable cells. Data presented as Mean ± SEM. $^*p < 0.05$, $^{**}p < 0.01$. (E) The variation of lymph nodes observed in control group and aLAG-3 group (left panel) and the size of lymph node was measured as indicated (right panel). Data presented as Mean ± SEM. $^{**}p < 0.01$. (F) Spleens were harvested for photograph from control group and aLAG-3 group (left panel). The spleen index was calculated as indicated (right panel). Data are presented as Mean ± SEM. $^{**}p < 0.01$, $^{***}p < 0.001$.

blockade of LAG-3 *in vivo*, which indicated the reversal of immune tolerance status (Figs. 5E and F). Our results revealed that the blockade of LAG-3 predominantly enhanced the $CD8^+$ T cell-mediated antitumor response in the HNSCC mouse model.

The blockade of LAG-3 reduced the population of immunosuppressive cells in HNSCC mouse model

On the basis of correlation of LAG-3 with immunosuppressive cells markers, we queried whether the blockade of LAG-3 impacted the number of Tregs, MDSCs and TAMs in HNSCC mouse model. As shown in Fig. 6A, the blockade of LAG-3 significantly decreased the population of $CD4^+Foxp3^+$ Tregs in HNSCC mouse model. For immature myeloid cells, we noted an increased count of $CD11b^+Gr1^+$ MDSCs and $CD11b^+F4/80^+$ TAMs in 2cKO tumor-bearing mice compared with WT mice, which is consistent with our previous study.[24] Here, we verified that the blockade of LAG-3 significantly reduced the amount of $CD11b^+Gr1^+$ MDSCs in spleen, lymph nodes and tumors using flow cytometry (Figs. 6B and C) and immunofluorescence (Fig. 6D) in aLAG-3 tumors of 2cKO mice. We also identified that the $CD11b^+F4/80^+$ TAMs significantly decreased in lymph nodes and tumors (Fig. 6E) but not in spleen (data not shown) and peripheral blood (data not shown). To identify the potential mediators of preferential accumulation of MDSCs and TAMs in 2cKO tumor-bearing mice, the expression of chemokines and cytokines in the serum was analyzed, revealing increased expression of multiple monocytes-attractive cytokines in the 2cKO tumor-bearing mice (Fig. 6F). The most differentially expressed monocytes-attractive cytokines were C5/C5a, G-CSF, IL-6, IL-13, CXCL1, M-CSF and CCL2 (quantified in Fig. 6G). Interestingly, the aLAG-3 tumor of 2cKO tumor-bearing mice appeared to exhibit markedly low levels of CXCL1 and CCL2 in comparison with controls (Fig. 6H), suggesting that the reduction of CXCL1 and CCL2 could be a part of factors that reduced the recruitment of immature myeloid cells. These data suggested that the blockade of LAG-3 led to the decrease population of Tregs and immature myeloid cells during antitumor immune response.

Discussion

Immune checkpoints, which limited the overactive immune response in normal immune system, were exploited to evade the host immune system in the tumor microenvironment.[30] LAG-3 was highly expressed on the dysfunctional or exhausted T cells that developed in tumor progression.[31] Here, we demonstrated the expression of LAG-3 was increased on TILs in human HNSCC, which indicated these cells were exhausted lymphocytes and confirmed the immunosuppressive status of HNSCC.[32] In addition, lacking of functional effector T cells subset may be a crucial reason for tumor progression, recurrence and metastasis, even similar total numbers of T cells presented around tumor.[33] This may suggest presence of LAG-3 in TILs facilitates tumor cell proliferation and resists eradicating tumor cells by the immune system, resulting in larger tumor and less differentiation in HNSCC. Many ongoing studies are exploring the effect of immune checkpoint inhibitors in recurrent and metastatic HNSCC, which include single agent and combination of immune checkpoint inhibitors as dual inhibition, combination with chemotherapy, radiotherapy, targeted agents as well as immunomodulators.[25] Here, our results demonstrated that LAG-3 was upregulated in recurrent HNSCC, metastatic lymph nodes and HNSCC with pre-radiotherapy. These findings provided a potential immunotherapeutic rationale that the efficiency of LAG-3 blockade coupled with or without radiotherapy should be evaluated in recurrent or metastatic HNSCC.

National Comprehensive Cancer Network (NCCN) clinical practice guidelines in oncology head and neck cancers are recommended to be approaches of treatment for HNSCC patients.[34] However, independent medical judge should not be ignored in the case of individual difference. Lymph node metastasis is one of the most significant prognosis factors of HNSCC patients, but treatment failure also occurs in patient with negative lymph node status.[35] Our present data indicated the expression of LAG-3 confers a poor prognosis in HNSCC patients with negative lymph node status. Hence, it may contribute to precisely individual treatment plan decision of node negative HNSCC patients. In addition, LAG-3 infiltration predicted poor survival in colorectal cancer and renal cell cancer.[36,37] In general, these results underlined the effect of LAG-3 impairing antitumor immunity in human HNSCC. However, keeping in mind that most of these cohorts are HPV- Chinese HNSCC patients, this may represent a subset of HNSCC. We also need to take into account that follow-up period was short and that prevents us from making cautious conclusion.

LAG-3 is expressed on T cells, B cells, natural killer cells, plasmacytoid dendritic cells (pDCs) and Tregs.[38,39] In consistent with previous studies, we found that the expression of LAG-3 identified a population of $CD4^+$ T cells, $CD8^+$ T cells and $CD4^+Foxp3^+$ Tregs, but not immature myeloid cells, in the HNSCC mouse model. *In vivo* study, LAG-3 blockade retarded tumor growth and significantly potentiated antitumor response of $CD8^+$ T cells. Current studies demonstrated that LAG-3 have direct and indirect role in $CD8^+$ T cells.[40] On one hand, the interaction between LAG-3 on $CD8^+$ T cells and LSECtin on tumor cells delivers a negative signal to downregulate T cells proliferation and cytokines production.[41] Thus, blockade of LAG-3 on $CD8^+$ T cells enhance $CD8^+$ T cells proliferation and response.[12] On the other hand, Tregs could induce activated T cells apoptosis, anergy and cell cycle arrest by cell-contact or secreting TGF-β1 and IL-10.[42] LAG-3 is expressed on Tregs and enhances the Tregs function.[20] Therefore, the blockade of LAG-3 reduces the population of Tregs and subsequently upregulates $CD8^+$ T cells. Curiously, the frequency of $CD4^+$ T cell could not be reinvigorated. Actually, the blockade of LAG-3 exhibited more persistent proliferation of $CD4^+$ T cells *in vitro*.[43] We hypothesis that the offset effect of the decreased frequency of $CD4^+$ $Foxp3^+$ Tregs and the increased frequency of $CD4^+$ T cells blocking with anti-LAG-3 antibody leads no detectable differences of $CD4^+$ T cells population.

Extensive analysis revealed a generalized increased of LAG-3 in many cell types, but our data found LAG-3 was almost negative in immature myeloid cells, including $CD11b^+Gr1^+$MDSCs

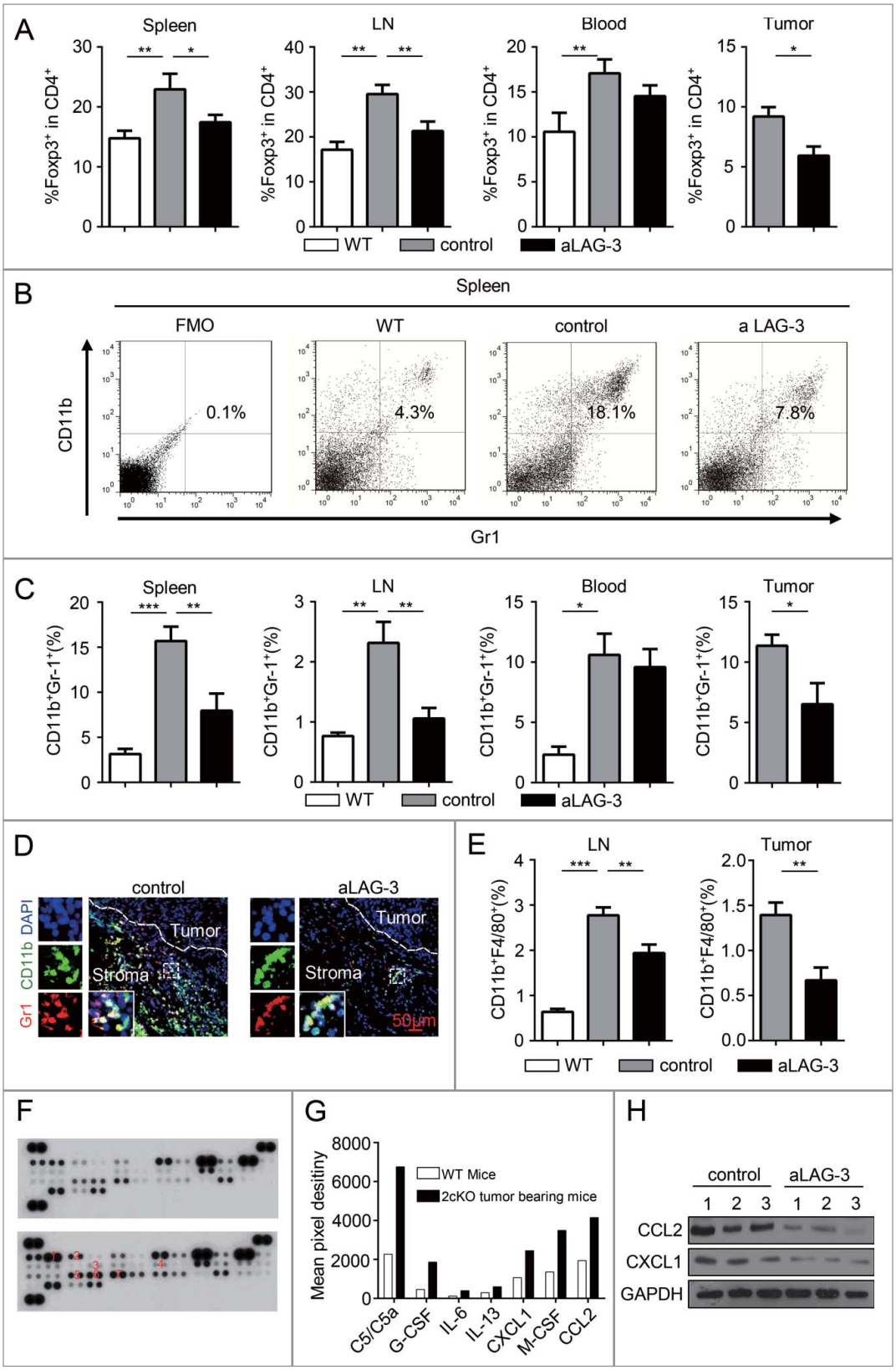

Figure 6. Blockade of LAG-3 reduced the population of immunosuppressive cells in HNSCC mouse model. (A) Quantification of the population of $Foxp3^+$ in $CD4^+$ T cells population from WT group, control group and aLAG-3 group. Cells were harvested from spleen, LN, peripheral blood and tumor tissues. Data shown as Mean ± SEM. $^*p$ <0 .05, $^{**}p$ <0 .01. (B) Flow cytometry plots and (C) quantification of $CD11b^+Gr1^+$ MDSCs in WT group, control group and aLAG-3 group. Cells were harvested from spleen, LN, peripheral blood and tumor tissues. Data presented as Mean ± SEM. $^*p < 0.05$, $^{**}p < 0.01$. (D) Representative immunofluorescence microscopy images of tumors stained with CD11b, Gr1 and DAPI in control mice and aLAG-3 mice. Scale bar, 50 μm. (E) Graphs from the flow cytometric analysis showing the percentage of TAMs ($CD11b^+F4/80^+$) in WT group, control group and aLAG-3 group. Cells were harvested from LN and tumor tissues. Data shown as Mean ± SEM. $^{**}p < 0.01$, $^{***}p <$ 0.001. (F) Cytokine antibody array showed the increased serum level of C5/C5a (1), G-CSF (2), IL-6 (3), IL-13 (4), CXCL1 (5), M-GSF (6), CCL2 (7) in WT mice and 2cKO tumor-bearing mice. (G)The mean pixel destiny of C5/C5a, G-CSF, IL-6, IL-13, CXCL1, M-GSF, CCL2 in WT mice and 2cKO tumor-bearing mice were calculated by Image Pro Plus 6.0 and normalized with reference spot. (H) CCL2 and CXCL1 expression levels were evaluated by Western blot in control group and aLAG-3 group.

and CD11b$^+$F4/80$^+$TAMs. Despite none of them expresses LAG-3, we were intrigued to find that the proportion of both MDSCs and TAMs was reduced after the blockade of LAG-3 *in vivo*. Indeed, we found a decrease level of CCL2 and CXCL1 in aLAG-3 2cKO mice. CCL2 could mediate recruitment of MDSCs to tumors and promote the function of MDSCs via STAT3 pathway.[44] And chemokine CXCL1, activated by IL-6, is also responsible for MDSCs accumulation.[45] Also, CCL2 and CXCL1 regulate the polarization of M1 macrophages to M2 phenotype and the recruitment of TAMs to tumor microenvironment.[46-48] The reduction of CCL2 and CXCL1 may support LAG-3 could impact the chemokine governing MDSCs and TAMs accumulation. Consistently, the blockade of LAG-3 results in pDC activation while reducing the level of CCL2 with subsequent limitation of MDSCs population.[39] Meanwhile, Tregs may also play an essential role in the recruitment of MDSCs and differentiation of TAMs, linking these immunosuppressive cells subsets in the tumor.[49] In addition, MDSCs and TAMs produce nitric oxide, reactive oxygen species and arginase 1, which induced desensitization of the T cells receptor (TCR) and T cells apoptosis.[50] Thus, additionally, the reduction of MDSCs and TAMs by LAG-3 blockade may partly conducive to the recovery of CD8$^+$ T cells.

In summary, our study reveals that LAG-3 is overexpressed on TILs, and its overexpression is correlated with the clinicopathological parameters and prognosis in human HNSCC. Using HNSCC mouse model, we elucidate that the blockade of LAG-3 restrains tumor progression. In addition, the blockade of LAG-3 also could strengthen immune reaction and improve immunosuppressive status in HNSCC mouse model in the tumor micro-environment and macro-environment. Although we evaluated the expression level of LAG-3 in human HNSCC samples and showed that targeting LAG-3 induces a significant antitumor immune response in HNSCC mouse model, it should be cautious assuming based on these findings that LAG-3 is a promising target. Taken together, these data suggest LAG-3 may be a potential target for immunotherapy in HNSCC.

Materials and methods

Mice

All animal proposals were approved and supervised by the Institutional Animal Care and Use Committee of Wuhan University. All animal studies were conducted in accordance with the NIH guidelines for the Care and Use of Laboratory Animals. The inducible head and neck tissue-specific *Tgfbr1*/*Pten* 2cKO mice (*Tgfbr1*$^{flox/flox}$; *Pten*$^{flox/flox}$; *K14-CreER*$^{tam+/-}$) were generated by crossing *K14-CreER*^{tam}; *Tgfbr1*$^{flox/flox}$ mice with *Pten*$^{flox/flox}$ mice.[27] The tissue-specific deletion of *Pten*, together with *Tgfbr1* in mice head and neck epithelia, causes multiple hyperproliferative and tumor lesions in head and neck area.[27] Deletion of *Pten* enhanced PI3K/Akt pathway activation in mouse head and neck epithelia.[27] And loss of *Tgfbr1* in head and neck epithelia, not in the stromal cells, enhances chemokine production, recruitment of tumor-promoting suppressor cells.[51] The mice maintained and genotyped as previously reported[29] and *Tgfbr1*$^{flox/flox}$/*Pten*$^{flox/flox}$ mice (*Tgfbr1*$^{flox/flox}$; *Pten*$^{flox/flox}$; *K14-CreER*$^{tam+/-}$) from same cage were separated as WT control. All the mice were bred in the FVBN/CD1/129/C57 mixed background.

Mouse cytokine antibody array

The Mouse Cytokine Antibody Array Panel A (*Proteome Profiler*^{TM} ARY006, R&D system) was applied to test the levels of serum cytokines of *Tgfbr1/Pten* 2cKO tumor-bearing mice as compared with WT mice counterpart (pooled with five mice, respectively). The pair of duplicate spots represented each cytokine and the average pixel density was determined by Image Pro Plus 6.0 (Cybernetics, Inc.) with subtract an averaged background signal.

In vivo LAG-3 antibody treatment

The *Tgfbr1/Pten* 2cKO mice were given tamoxifen by oral gavage for five consequent days.[52] And these mice randomly were divided into two groups. A week later, isotype control (control group, *in vivo* MAb mouse IgG1 isotype control, Clone: MOPC-21; Bioxcell; n = 6 mice; 10 mg/kg) or anti-mouse LAG-3 group (aLAG-3 group, *in vivo* mAb LAG-3 antibody, Clone: C9B7W, Bioxcell; n = 6 mice; 10 mg/kg) was intraperitoneally injected into *Tgfbr1/Pten* 2cKO mice every other day in next 10 d. The endpoint was determined according to a systematic evaluation by the veterinarian. Photographs of tumor-bearing mice were taken at day 32 and day 40 and body weight was measured every other day. The tumor volumes were calculated by micrometer caliper every 5 d. All mice were euthanized at the end of the study.

Flow cytometry

Single-cell suspension isolated from spleen, lymph nodes, peripheral blood and tumors was acquired as previously described.[24] These cells from different groups including WT and 2cKO tumor-bearing mice treated with isotype or anti-m LAG-3 monoclonal antibody resuspended in staining buffer (PBS with 2% FBS) at 4°C and non-specific Fc was blocking for 10 min at 4°C. Fluorochrome-conjugated monoclonal antibodies were used to staining: isotype-matched IgG controls, Percp-Cy5.5-conjugated F4/80 and Foxp3 (eBioscience), PE-conjugated LAG-3, IFNγ (eBioscience), FITC-conjugated CD4$^+$, CD8$^+$ and CD11b (eBioscience), PE-Cy7-conjugated Gr1 (BD). For intracellular IFNγ staining, the Cell Stimulation Cocktail (plus protein transport inhibitors, eBioscience), including phorbol 12-myristate 13-acetate (PMA), ionomycin, brefeldin A and monensin, was used for induction and subsequent intracellular detection of IFNγ. Death cells were excluded by staining 7AAD (Invitrogen). Isotype control and positive control were set for each antibody and each experiment. Different gating strategy was used to identify the cell populations. Data were analyzed with Flowjo 7.6 (Tree Star).

Human HNSCC tissue samples

Human HNSCC tissue samples included 27 normal mucosa, 43 dysplasia (Dys), 122 primary HNSCC, 8 recurrent HNSCC, 41

metastatic lymph nodes, 12 HNSCC with preradiotherapy history and 11 HNSCC with inductive TPF chemotherapy. Immunohistochemical staining of p16 and HPV DNA *in situ* hybridization technique were used to monitor HPV infection as previously reported.[24] All tissue samples were obtained from surgically resected patients in the Department of Oral and Maxillofacial Surgery, School and Hospital of Stomatology Wuhan University. The School and Hospital of Stomatology of Wuhan University Medical Ethics Committee approved this study, and informed consent was obtained from the patients before they underwent surgery. The clinical stages of their HNSCC were classified according to the guidelines of the International Union Against Cancer (UICC 2002), and histological grading was determined according to the scheme of the World Health Organization. The 11 HNSCC patients receive two round combined cisplatin, docetaxel and 5-fuorouracil (TPF) therapy with the same protocol of Zhang's clinical trial (NCT01542931).[53]

Immunohistochemistry

Paraffin sections of tumor tissue were rehydration and antigen retrieval was performed in sodium citrate. The 3% hydrogen peroxide was applied to block-up endogenous peroxidase. Antigen retrieval was performed in sodium citrate in a pressure cooker. Then, the incubation of goat serum was used to block the non-specific binding at 37°C for 1 h. Next, sections were incubated with antibody for LAG-3 (Abcam), $CD8^+$ (Zymed), Foxp3 (CST), CD68 (Zymed), CD163 (CWBiotech) CD11b (Abcam), CD33 (Zymed) and p16 (Zymed) (4°C overnight). Sections were incubated with secondary biotinylated immunoglobulin G antibody solution and an avidin-biotin-peroxidase reagent. At last, the section stained with DAB kit (Mxb Bio) and the sections lightly counterstained with haematoxylin (Invitrogen, USA). Negative control with primary antibody replaced by PBS and commercial available positive control for each antibody were set in parallel. The immunohistochemical method of mouse sections was followed as described above.

Immunofluorescence

Immunofluorescence was carried out as previously described.[28] For staining of LAG-3, the human tissue samples were fixed by 4% paraformaldehyde and embedded in paraffin. Sections were hydrated in alcohol and antigen retrieval was performed in sodium citrate in a pressure cooker. Then sections were blocked with goat serum for 1 h at 37°C and incubated with LAG3 antibody (GeneTex) at 4°C overnight at indicated dilution. Next day, sections were incubated with fluorochrome conjugated secondary antibodies (Alexa 594 anti-rabbit; Invitrogen) for 1 h at 37°C protected from the light and DPAI (Vector Laboratories) was used as the nuclear counterstain. Confocal images were taken with C2+ confocal microscope system (Nikon). For staining of MDSCs, mouse tumor tissues (4 Âμm thick) were treated as described above and incubated with anti-CD11b antibody (Abcam) and anti-mouse Ly-6G/Ly-6C (Gr-1) (BioLegend). Then, sections were incubated with secondary antibodies (Alexa 594 anti-rat and Alexa 488 anti-rabbit; Invitrogen). Fluorescence images were taken with CLSM-310, Zeiss fluorescence microscope.

Western blot

The mouse tumor tissue was carefully dissected (n = 6 mice, respectively) and storage at −80°C. All samples were lysed with RIPA Lysis Buffer (Beyotime), which contains protease inhibitor and phosphatase inhibitors, and sonicated after centrifugation. Lysates were denatured in loading buffer (Beyotime) and separated by 12% SDS-polyacrylamide gel electrophoresis and protein transferred to polyvinylidene fluoride membranes (Millipore Corporation). The primary antibodies used in Western blot were as follows: mouse LAG-3 antibody (R&D), CXCL1 antibody (GeneTex) and CCL2 antibody (Novus). GAPDH was used as loading control. Enhanced chemiluminescence detection kit (Advansta) was applied to Western blot staining. All Western blots were repeated at least three times.

Scoring system

Aperio ScanScope CS scanner was exploited for scanning all slices and quantifying the histoscore of each sample with background subtraction as previously described.[29] The scanner of each slice was quantified with Aperio Quantification System (Version 9.1).

Statistical analysis

Statistical analysis was carried out using GraphPad Prism 6.0 (Graph Pad Software Inc.). Difference among three groups was analyzed by One-way ANOVO followed Tukey test. Difference between two groups was analyzed by un-paired or paired *t* test. The data are presented as the Mean ± SEM, and statistical significance was determined as $p < 0.05$. The correlation was evaluated by Two-tailed Pearson's statistics. The Kaplan–Meier method and the log-rank test were used to analyze the univariate analysis of OS by Graphpad Prism 6.0. The Cox proportional hazards regression model was used to evaluate the multivariate analyses for OS by SPSS 22.0 (IBM). The hierarchical analysis was carried out as described previously.[54]

Disclosure of potential conflicts of interest

No potential conflicts of interest were disclosed.

Funding

This work was supported by National Natural Science Foundation of China 81272963, 81472528, 81672668 (Z.J. Sun), 81272964, 81472529 (W. F. Zhang), and the Division of Intramural Research, NIDCR, NIH, USA (A.B. Kulkarni). Z. J. Sun was supported by program for New Century Excellent Talents in University (NCET-13-0439), Ministry of Education of China.

References

1. Jemal A, Bray F, Center MM, Ferlay J, Ward E, Forman D. Global cancer statistics. CA Cancer J Clin 2011; 61:69-90; PMID:21296855; http://dx.doi.org/10.3322/caac.20107
2. Mao L, Hong WK, Papadimitrakopoulou VA. Focus on head and neck cancer. Cancer Cell 2004; 5:311-6; PMID:15093538; http://dx.doi.org/10.1016/S1535-6108(04)00090-X
3. Economopoulou P, Kotsantis I, Psyrri A. Checkpoint Inhibitors in Head and Neck Cancer: Rationale, Clinical Activity, and Potential Biomarkers. Curr Treat Options Oncol 2016; 17:40; PMID:27315066; http://dx.doi.org/10.1007/s11864-016-0419-z
4. Bauman JE, Ferris RL. Integrating novel therapeutic monoclonal antibodies into the management of head and neck cancer. Cancer 2014; 120:624-32; PMID:24222079; http://dx.doi.org/10.1002/cncr.28380
5. Hodi FS, O'Day SJ, McDermott DF, Weber RW, Sosman JA, Haanen JB, Gonzalez R, Robert C, Schadendorf D, Hassel JC et al. Improved survival with ipilimumab in patients with metastatic melanoma. N Engl J Med 2010; 363:711-23; PMID:20525992; http://dx.doi.org/10.1056/NEJMoa1003466
6. Wolchok JD, Kluger H, Callahan MK, Postow MA, Rizvi NA, Lesokhin AM, Segal NH, Ariyan CE, Gordon RA, Reed K et al. Nivolumab plus ipilimumab in advanced melanoma. N Engl J Med 2013; 369:122-33; PMID:23724867; http://dx.doi.org/10.1056/NEJMoa1302369
7. Anderson AC, Joller N, Kuchroo VK. Lag-3, Tim-3, and TIGIT: co-inhibitory receptors with specialized functions in immune regulation. Immunity 2016; 44:989-1004; PMID:27192565; http://dx.doi.org/10.1016/j.immuni.2016.05.001
8. Huard B, Prigent P, Tournier M, Bruniquel D, Triebel F. CD4/major histocompatibility complex class II interaction analyzed with CD4- and lymphocyte activation gene-3 (LAG-3)-Ig fusion proteins. Eur J Immunol 1995; 25:2718-21; PMID:7589152; http://dx.doi.org/10.1002/eji.1830250949
9. Liu W, Tang L, Zhang G, Wei H, Cui Y, Guo L, Gou Z, Chen X, Jiang D, Zhu Y et al. Characterization of a novel C-type lectin-like gene, LSECtin: demonstration of carbohydrate binding and expression in sinusoidal endothelial cells of liver and lymph node. J Biol Chem 2004; 279:18748-58; PMID:14711836; http://dx.doi.org/10.1074/jbc.M311227200
10. Xu F, Liu J, Liu D, Liu B, Wang M, Hu Z, Du X, Tang L, He F. LSECtin expressed on melanoma cells promotes tumor progression by inhibiting antitumor T-cell responses. Cancer Res 2014; 74:3418-28; PMID:24769443; http://dx.doi.org/10.1158/0008-5472.CAN-13-2690
11. Matsuzaki J, Gnjatic S, Mhawech-Fauceglia P, Beck A, Miller A, Tsuji T, Eppolito C, Qian F, Lele S, Shrikant P et al. Tumor-infiltrating NY-ESO-1-specific CD8+ T cells are negatively regulated by LAG-3 and PD-1 in human ovarian cancer. Proc Natl Acad Sci U S A 2010; 107:7875-80; PMID:20385810; http://dx.doi.org/10.1073/pnas.1003345107
12. Grosso JF, Kelleher CC, Harris TJ, Maris CH, Hipkiss EL, De Marzo A, Anders R, Netto G, Getnet D, Bruno TC et al. LAG-3 regulates CD8+ T cell accumulation and effector function in murine self- and tumor-tolerance systems. J Clin Invest 2007; 117:3383-92; PMID:17932562; http://dx.doi.org/10.1172/JCI31184
13. Woo SR, Turnis ME, Goldberg MV, Bankoti J, Selby M, Nirschl CJ, Bettini ML, Gravano DM, Vogel P, Liu CL et al. Immune inhibitory molecules LAG-3 and PD-1 synergistically regulate T-cell function to promote tumoral immune escape. Cancer Res 2012; 72:917-27; PMID:22186141; http://dx.doi.org/10.1158/0008-5472.CAN-11-1620
14. Huang RY, Eppolito C, Lele S, Shrikant P, Matsuzaki J, Odunsi K. LAG3 and PD1 co-inhibitory molecules collaborate to limit CD8+ T cell signaling and dampen antitumor immunity in a murine ovarian cancer model. Oncotarget 2015; 6:27359-77; PMID:26318293; http://dx.doi.org/10.18632/oncotarget.4751
15. Ferris RL. Immunology and immunotherapy of head and neck cancer. J Clin Oncol 2015; 33:3293-304; PMID:26351330; http://dx.doi.org/10.1200/JCO.2015.61.1509
16. Weed DT, Vella JL, Reis IM, De la Fuente AC, Gomez C, Sargi Z, Nazarian R, Califano J, Borrello I, Serafini P. Tadalafil reduces myeloid-derived suppressor cells and regulatory T cells and promotes tumor immunity in patients with head and neck squamous cell carcinoma. Clin Cancer Res 2015; 21:39-48; PMID:25320361; http://dx.doi.org/10.1158/1078-0432.CCR-14-1711
17. Ostrand-Rosenberg S, Sinha P. Myeloid-derived suppressor cells: linking inflammation and cancer. J Immunol 2009; 182:4499-506; PMID:19342621; http://dx.doi.org/10.4049/jimmunol.0802740
18. Strauss L, Bergmann C, Gooding W, Johnson JT, Whiteside TL. The frequency and suppressor function of CD4+CD25highFoxp3+ T cells in the circulation of patients with squamous cell carcinoma of the head and neck. Clin Cancer Res 2007; 13:6301-11; PMID:17975141; http://dx.doi.org/10.1158/1078-0432.CCR-07-1403
19. Komohara Y, Jinushi M, Takeya M. Clinical significance of macrophage heterogeneity in human malignant tumors. Cancer Sci 2014; 105:1-8; PMID:24168081; http://dx.doi.org/10.1111/cas.12314
20. Huang CT, Workman CJ, Flies D, Pan X, Marson AL, Zhou G, Hipkiss EL, Ravi S, Kowalski J, Levitsky HI et al. Role of LAG-3 in regulatory T cells. Immunity 2004; 21:503-13; PMID:15485628; http://dx.doi.org/10.1016/j.immuni.2004.08.010
21. Network CGA. Comprehensive genomic characterization of head and neck squamous cell carcinomas. Nature 2015; 517:576-82; PMID:25631445; http://dx.doi.org/10.1038/nature14129
22. Rhodes DR, Kalyana-Sundaram S, Mahavisno V, Varambally R, Yu J, Briggs BB, Barrette TR, Anstet MJ, Kincead-Beal C, Kulkarni P et al. Oncomine 3.0: genes, pathways, and networks in a collection of 18,000 cancer gene expression profiles. Neoplasia 2007; 9:166-80; PMID:17356713; http://dx.doi.org/10.1593/neo.07112
23. Gillison ML, Koch WM, Capone RB, Spafford M, Westra WH, Wu L, Zahurak ML, Daniel RW, Viglione M, Symer DE et al. Evidence for a causal association between human papillomavirus and a subset of head and neck cancers. J Natl Cancer Inst 2000; 92:709-20; PMID:10793107; http://dx.doi.org/10.1093/jnci/92.9.709
24. Yu GT, Bu LL, Huang CF, Zhang WF, Chen WJ, Gutkind JS, Kulkarni AB, Sun ZJ. PD-1 blockade attenuates immunosuppressive myeloid cells due to inhibition of CD47/SIRPalpha axis in HPV negative head and neck squamous cell carcinoma. Oncotarget 2015; 6:42067-80; PMID:26573233; http://dx.doi.org/10.18632/oncotarget.5955.
25. Sadraei NH, Sikora AG, Brizel DM. Immunotherapy and checkpoint inhibitors in recurrent and metastatic head and neck cancer. Am Soc Clin Oncol Educ Book 2016; 35:e277-82; PMID:27249733; http://dx.doi.org/10.14694/EDBK_157801
26. Molinolo AA, Amornphimoltham P, Squarize CH, Castilho RM, Patel V, Gutkind JS. Dysregulated molecular networks in head and neck carcinogenesis. Oral Oncol 2009; 45:324-34; PMID:18805044; http://dx.doi.org/10.1016/j.oraloncology.2008.07.011
27. Bian Y, Hall B, Sun ZJ, Molinolo A, Chen W, Gutkind JS, Waes CV, Kulkarni AB. Loss of TGF-β signaling and PTEN promotes head and neck squamous cell carcinoma through cellular senescence evasion and cancer-related inflammation. Oncogene 2012; 31:3322-32; PMID:22037217; http://dx.doi.org/10.1038/onc.2011.494
28. Yu GT, Bu LL, Zhao YY, Mao L, Deng WW, Wu TF, Zhang WF, Sun ZJ. CTLA4 blockade reduces immature myeloid cells in head and neck squamous cell carcinoma. Oncoimmunology 2016; 5:e1151594; PMID:27471622; http://dx.doi.org/10.1080/2162402X.2016.1151594
29. Sun ZJ, Zhang L, Hall B, Bian Y, Gutkind JS, Kulkarni AB. Chemopreventive and chemotherapeutic actions of mTOR inhibitor in genetically defined head and neck squamous cell carcinoma mouse model. Clin Cancer Res 2012; 18:5304-13; PMID:22859719; http://dx.doi.org/10.1158/1078-0432.CCR-12-1371
30. Pardoll DM. The blockade of immune checkpoints in cancer immunotherapy. Nat Rev Cancer 2012; 12:252-64; PMID:22437870; http://dx.doi.org/10.1038/nrc3239
31. Sierro S, Romero P, Speiser DE. The CD4-like molecule LAG-3, biology and therapeutic applications. Expert Opin Ther Targets 2011; 15:91-101; PMID:21142803; http://dx.doi.org/10.1517/14712598.2011.540563
32. Kuss I, Hathaway B, Ferris RL, Gooding W, Whiteside TL. Decreased absolute counts of T lymphocyte subsets and their relation to disease in squamous cell carcinoma of the head and neck. Clin Cancer Res 2004; 10:3755-62; PMID:15173082; http://dx.doi.org/10.1158/1078-0432.CCR-04-0054

33. Camus M, Tosolini M, Mlecnik B, Pages F, Kirilovsky A, Berger A, Costes A, Bindea G, Charoentong P, Bruneval P et al. Coordination of intratumoral immune reaction and human colorectal cancer recurrence. Cancer Res 2009; 69:2685-93; PMID:19258510; http://dx.doi.org/10.1158/0008-5472.CAN-08-2654
34. Pfister DG, Spencer S, Brizel DM, Burtness B, Busse PM, Caudell JJ, Cmelak AJ, Colevas AD, Dunphy F, Eisele DW et al. Head and neck cancers, Version 2.2014. Clinical practice guidelines in oncology. J Natl Compr Canc Netw 2014; 12:1454-87; PMID:25313184
35. Keski-Santti H, Atula T, Tornwall J, Koivunen P, Makitie A. Elective neck treatment versus observation in patients with T1/T2 N0 squamous cell carcinoma of oral tongue. Oral Oncol 2006; 42:96-101; PMID:16256414; http://dx.doi.org/10.1016/j.oraloncology.2005.06.018
36. Chen J, Chen Z. The effect of immune microenvironment on the progression and prognosis of colorectal cancer. Med Oncol 2014; 31:82; PMID:25034363; http://dx.doi.org/10.1007/s12032-014-0082-9
37. Giraldo NA, Becht E, Pages F, Skliris G, Verkarre V, Vano Y, Mejean A, Saint-Aubert N, Lacroix L, Natario I et al. Orchestration and Prognostic Significance of Immune Checkpoints in the Microenvironment of Primary and Metastatic Renal Cell Cancer. Clin Cancer Res 2015; 21:3031-40; PMID:25688160; http://dx.doi.org/10.1158/1078-0432.CCR-14-2926
38. Topalian SL, Drake CG, Pardoll DM. Immune checkpoint blockade: a common denominator approach to cancer therapy. Cancer Cell 2015; 27:450-61; PMID:25858804; http://dx.doi.org/10.1016/j.ccell.2015.03.001
39. Castelli C, Triebel F, Rivoltini L, Camisaschi C. Lymphocyte activation gene-3 (LAG-3, CD223) in plasmacytoid dendritic cells (pDCs): a molecular target for the restoration of active antitumor immunity. Oncoimmunology 2014; 3:e967146; PMID:25941596; http://dx.doi.org/10.4161/21624011.2014.967146
40. Workman CJ, Vignali DA. Negative regulation of T cell homeostasis by lymphocyte activation gene-3 (CD223). J Immunol 2005; 174:688-95; PMID:15634887; http://dx.doi.org/10.4049/jimmunol.174.2.688
41. Do JS, Valujskikh A, Vignali DA, Fairchild RL, Min B. Unexpected role for MHC II-peptide complexes in shaping CD8 T-cell expansion and differentiation in vivo. Proc Natl Acad Sci U S A 2012; 109:12698-703; PMID:22802622; http://dx.doi.org/10.1073/pnas.1207219109
42. Alhamarneh O, Amarnath SM, Stafford ND, Greenman J. Regulatory T cells: what role do they play in antitumor immunity in patients with head and neck cancer? Head Neck 2008; 30:251-61; PMID:18172882; http://dx.doi.org/10.1002/hed.20739
43. Huard B, Tournier M, Hercend T, Triebel F, Faure F. Lymphocyte-activation gene 3/major histocompatibility complex class II interaction modulates the antigenic response of CD4+ T lymphocytes. Eur J Immunol 1994; 24:3216-21; PMID:7805750; http://dx.doi.org/10.1002/eji.1830241246
44. Chun E, Lavoie S, Michaud M, Gallini CA, Kim J, Soucy G, Odze R, Glickman JN, Garrett WS. CCL2 promotes colorectal carcinogenesis by enhancing polymorphonuclear myeloid-derived suppressor cell population and function. Cell Rep 2015; 12:244-57; PMID:26146082; http://dx.doi.org/10.1016/j.celrep.2015.06.024
45. Sander LE, Sackett SD, Dierssen U, Beraza N, Linke RP, Muller M, Blander JM, Tacke F, Trautwein C. Hepatic acute-phase proteins control innate immune responses during infection by promoting myeloid-derived suppressor cell function. J Exp Med 2010; 207:1453-64; PMID:20530204; http://dx.doi.org/10.1084/jem.20091474
46. Zarif JC, Taichman RS, Pienta KJ. TAM macrophages promote growth and metastasis within the cancer ecosystem. Oncoimmunology 2014; 3:e941734; PMID:25954596; http://dx.doi.org/10.4161/21624011.2014.941734
47. Remus EW, Sayeed I, Won S, Lyle AN, Stein DG. Progesterone protects endothelial cells after cerebrovascular occlusion by decreasing MCP-1- and CXCL1-mediated macrophage infiltration. Exp Neurol 2015; 271:401-8; PMID:26188381; http://dx.doi.org/10.1016/j.expneurol.2015.07.010
48. Balkwill FR. The chemokine system and cancer. J Pathol 2012; 226:148-57; PMID:21989643; http://dx.doi.org/10.1002/path.3029
49. Holmgaard RB, Zamarin D, Li Y, Gasmi B, Munn DH, Allison JP, Merghoub T, Wolchok JD. Tumor-expressed IDO recruits and activates MDSCs in a Treg-dependent manner. Cell Rep 2015; 13:412-24; PMID:26411680; http://dx.doi.org/10.1016/j.celrep.2015.08.077
50. Gabrilovich DI, Ostrand-Rosenberg S, Bronte V. Coordinated regulation of myeloid cells by tumours. Nat Rev Immunol 2012; 12:253-68; PMID:22437938; http://dx.doi.org/10.1038/nri3175
51. Bian Y, Terse A, Du J, Hall B, Molinolo A, Zhang P, Chen W, Flanders KC, Gutkind JS, Wakefield LM et al. Progressive tumor formation in mice with conditional deletion of TGF-β signaling in head and neck epithelia is associated with activation of the PI3K/Akt pathway. Cancer Res 2009; 69:5918-26; PMID:19584284; http://dx.doi.org/10.1158/0008-5472.CAN-08-4623
52. Zhang L, Sun ZJ, Bian Y, Kulkarni AB. MicroRNA-135b acts as a tumor promoter by targeting the hypoxia-inducible factor pathway in genetically defined mouse model of head and neck squamous cell carcinoma. Cancer Lett 2013; 331:230-8; PMID:23340180; http://dx.doi.org/10.1016/j.canlet.2013.01.003
53. Zhong LP, Zhang CP, Ren GX, Guo W, William WN, Jr, Sun J, Zhu HG, Tu WY, Li J, Cai YL et al. Randomized phase III trial of induction chemotherapy with docetaxel, cisplatin, and fluorouracil followed by surgery versus up-front surgery in locally advanced resectable oral squamous cell carcinoma. J Clin Oncol 2013; 31:744-51; PMID:23129742; http://dx.doi.org/10.1200/JCO.2012.43.8820
54. Huang CF, Zhang L, Ma SR, Zhao ZL, Wang WM, He KF, Zhao YF, Zhang WF, Liu B, Sun ZJ. Clinical significance of Keap1 and Nrf2 in oral squamous cell carcinoma. PLoS One 2013; 8:e83479; PMID:24386210; http://dx.doi.org/10.1371/journal.pone.0083479